Shear deformation of polymer melt observed via proton NMR: Theory and experiment

B. S. Douglass, R. J. Cormier, and P. T. Callaghan*
MacDiarmid Institute for Advanced Materials and Nanotechnology, School of Chemical and Physical Sciences, Victoria University of Wellington, Wellington, New Zealand

(Received 15 November 2006; revised manuscript received 25 January 2007; published 16 April 2007)

We here develop a theory for the effect of shearing flow on residual proton dipole-dipole interactions for polymer melts. The model is based on the use of correlation functions which derive from the return to origin probability for polymers reptating in the tube of surrounding constraints. Using Doi-Edwards theory we calculate the spin-echo response under equilibrium conditions and then consider the effect of a shearing flow which deforms the tube, finding that there exists a strong dependence of transverse relaxation on Weissenberg number. The results are compared with NMR measurements of shear-perturbed proton T_2 relaxation in 494 kDa poly (dimethylsiloxane).

DOI: 10.1103/PhysRevE.75.041802 PACS number(s): 83.80.Sg, 83.85.Rx, 83.80.Va, 76.60.−k

I. INTRODUCTION

In one of the earliest "Rheo-NMR" experiments [1] Nakatani *et al.* placed a polysiloxane melt in a Couette cell and observed the proton NMR line shape under steady shear flow. The idea behind the method was that shear-induced order and consequent anisotropic segmental reorientation could result in residual proton-proton dipolar interactions. In that experiment the linewidth was unperturbed, probably due to the deformation being insufficient to yield a strain rate consistent with significant polymer deformation. Nonetheless, this first venture was a precursor to many subsequent experimental studies [2–6] of NMR spectra in deformational flow. Later Rheo-NMR experiments on sheared polymer melts have indicated linewidth changes [2], as revealed by faster spin-spin relaxation. However lack of a suitable theory connecting the spin-relaxation rate to statistical physics models of the polymer deformation has made such measurements difficult to interpret. A much easier interpretation is possible in the case of deuteron NMR measurements where the use of a small deuterated probe molecule permits a direct measurement of the ensemble-averaged segmental alignment tensor, a quantity predicted in detail by Doi-Edwards theory [7] and its subsequent variants [8]. This is possible both because the deuterium quadrupole interaction has a simple dependence on the local probe molecule orientation and because rapid diffusion of the probe as it collides with successive polymer segments leads to an ensemble-averaged orientation inherited from the host, as expressed through the motionally averaged quadrupolar Hamiltonian. The deuteron method has proven highly effective in Rheo-NMR measurements of the segmental alignment tensor for a wide range of molecular weights in poly(dimethylsiloxane) melts [9–11].

Despite the success of the deuteron NMR method, there are a number of reasons why use of proton NMR is advantageous. These include the much greater proton NMR sensitivity, the abundance of protons in most polymers, and the absence of any modification of melt rheology due to the presence of a potentially plasticizing probe molecule. For this reason we have attempted here to derive a theory which connects the Doi-Edwards predictions for segmental alignment to the residual proton-proton dipolar interaction as measured in a simple spin-echo experiment. Such an experiment yields the rate at which protons lose transverse magnetization due to loss of phase coherence. The time constant associated with this rate is called T_2 [12]. We will show, by comparison with measurements carried out in a Couette cell, that the theory gives a good representation of the apparent spin-spin relaxation time as a function of applied steady shear rate.

The essential physics behind our theory is as follows. First, we postulate an average dipolar interaction strength as given by the second moment of the dipolar frequency distribution experienced by polymer segments undergoing equilibration dynamics within the local tube formed by the topological constraints of neighboring chains. We further allow that this interaction strength will vary with the degree of local stretching of the polymer chain, as given by the usual Gaussian distribution of end-to-end distances. Second, that part of the tube local to the polymer segment (the "tube step") will have a particular orientation which is lost only by reptation of the ends of the polymer past that step in the tube renewal process. Consequently the dipolar interaction is projected into the laboratory frame, as defined by the magnetic field direction, according to the usual second rank Legendre polynomial $\frac{1}{2}(3\cos^2\theta-1)$, where θ is the polar angle between the tube step vector and the magnetic field. We use the Doi-Edwards model to calculate the shear dependence of the distribution of tube step orientations. Unlike the case of a deuterated probe molecule, we do not sample an ensemble-averaged Hamiltonian since the protons are attached to their local polymer segments in their local tube step. Instead we detect a sum of NMR signals contributed by protons residing in each of those steps. Finally we allow for the fluctuation of the dipolar frequency, $\omega_d(t)$, as segments reptate between tube steps and hence different local dipolar interaction projections. Our treatment is based on an earlier idea by Ball, Callaghan and Samulski (BCS) [13] by which a dipolar correlation function for polymer melts in equilibrium may be derived by considering the "return to origin" (RTO) probability as polymer segments reptate around the distribution of

*Electronic address: paul.callaghan@vuw.ac.nz

tube steps. Callaghan and Samulski [3] applied that model in a study of proton dipolar relaxation in poly (dimethylsiloxane) melts under zero shear conditions, showing in the process that polymer tube disengagement times and their dependence on molar mass were consistent with the Doi-Edwards model [7,14]. That zero-shear RTO must now be suitably modified to allow for a nonisotropic step orientation distribution. In particular we no longer obtain a zero correlation for segments not returning to tube step origin when the polymer is deformed.

This paper is organized as follows. First we describe the BCS model for dipolar interactions under reptation, but now explicitly include the non-RTO probability which, in the shear deformation case, can yield finite correlations. Next we express the shear deformation tensor in the hydrodynamic frame using the usual independent alignment approximation, allowing us to calculate the form of the dipolar relaxation function as a function of shear rate. Finally we express this relaxation function for the special cases of the magnetic field being aligned along the vorticity, gradient, and velocity directions. The experimental section describes the polymer used, the Couette cell and the NMR apparatus. It also describes how the use of spatially selective rf pulses allows one to choose the relevant hydrodynamic direction along which to project the dipolar interaction. The results section compares the experimental results with our theoretical projections. Free parameters in the fit are the tube disengagement time and the dipolar interaction strength and we show here that the values derived from our fit are consistent with other NMR measurements.

II. THEORY

Our first step in outlining the theory is to consider the interaction experienced by a nuclear spin located in a polymer segment undergoing rapid reorientational motions, those motions being constrained by the entanglements due to neighboring chains. The reorientational motions cause the internuclear dipolar interactions to fluctuate and our task is to see how those constrained motions are reflected in the nuclear spin relaxation, and then to determine what effect a shear deformation will have on that relaxation process. In doing so we will use the polymer physics model of Doi and Edwards (DE) which has proven successful in linking the molecular or microscopic properties of entangled high molecular weight random coil polymers to macroscopically observable properties. DE utilizes the instantaneous mean-field approach whereby each polymer diffuses in a tube formed by neighboring chains. At length scales smaller than the tube diameter, a, polymer segments undergo rapid equilibrational (Rouse) dynamics constrained only by segment connectivity. Beyond a the Rouse dynamics are confined to curvilinear displacements (reptation) along the tube, the final dynamics arising from the dissipation of the tubes themselves and the creation of new tubes as polymers reptate. Hence in the DE model, the hierarchy of motion is as follows. The characteristic time taken for a monomer to diffuse, in Rouse motion, the distance between entanglements a is the equilibration time τ_e. The intermediate characteristic time τ_R corresponds to the time taken for the polymer to diffuse its rms end-to-end distance in the curvilinear tube path. τ_d is the tube disengagement time, the final relaxation time characterizing tube dissipation.

The equilibration modes are so fast compared with the strength of the dipolar interaction expressed in frequency units, that the dipolar interactions are effectively averaged over the equilibration mode time scales. This has the effect of diminishing, but not entirely removing, the effective dipole-dipole interaction. But as the slower curvilinear reptational and tube dissipation processes cause the remaining dipolar interaction to further fluctuate, the NMR measurement is able to access the dynamics.

A. Dipolar relaxation function for reptating polymer segments in the absence of shear

1. The dipolar interaction

For magnetic resonance in soft matter, the Zeeman interaction between a nuclear spin and the magnetic field in which it is immersed usually overwhelmingly dominates the various weaker but important contributions to the nuclear spin Hamiltonian arising from local interactions of the spin with its environment. The particular local interaction which will concern us is the internuclear, homonuclear dipolar interaction. The sum of all through-space dipole-dipole interactions between one spin and its neighbors plays the major role in determining the transverse relaxation of the magnetization of nuclei within a polymer sample.

The dipolar interaction is described by an inner product of rank-2 spatial and spin operators and the Hamiltonian contribution of the interaction between two spins (labelled 1 and 2) separated by an internuclear distance r_{12} can be written as

$$H_D(t) = \frac{-\mu_0\gamma^2\hbar}{4\pi r_{12}^3}\sum_m (-1)^m \left(\frac{24\pi}{5}\right)^{1/2} Y_2^m(\Theta(t),\Phi(t))T_2^m, \tag{1}$$

where the Y_2^m are spherical harmonics of order 2 and component m, while the T_2^m are bilinear products of spin operators [17]. The angles Θ and Φ refer to the orientation of the internuclear vector with respect to the main polarizing field, and as such will fluctuate as the spins diffuse about throughout the characteristic time scales.

Off-diagonal components of the above tensor representation contribute to transitions between eigenstates and hence primarily to the longitudinal T_1 or spin-lattice relaxation process, a phenomenon that while useful, will not be of further application here. However, the secular components of this dipolar perturbation to the Hamiltonian influence the precessional frequencies of the spin coherences and thereby contribute to the transverse relaxation associated with dephasing. The secular part of the dipolar interaction tensor may be written as

$$H_{D0}(t) = \frac{\mu_0\gamma^2\hbar}{4\pi r_{12}^3} P_2[\cos\Theta(t)][3I_{1z}I_{2z} - \mathbf{I}_1\cdot\mathbf{I}_2], \tag{2}$$

where $P_2(\cos\Theta)$ is the second-order Legendre polynomial $\frac{3}{2}(\cos^2\Theta - \frac{1}{3})$. Dipolar perturbations such as these induce ad-

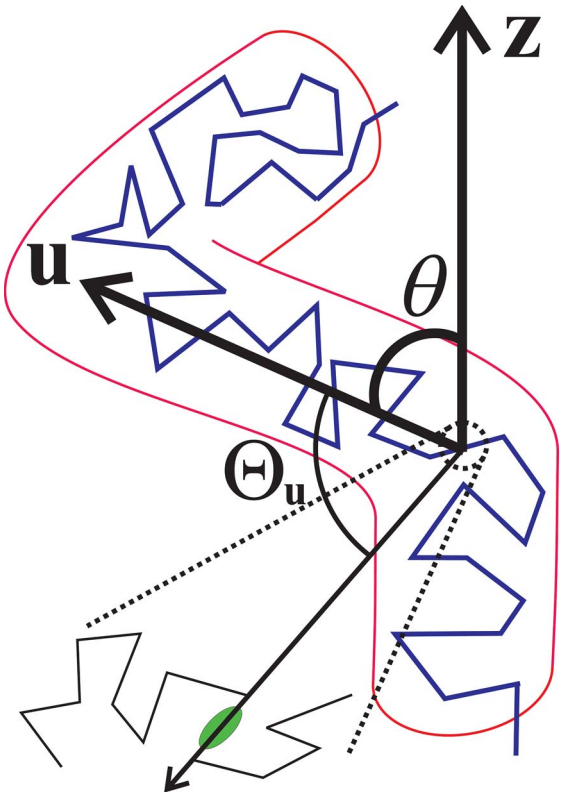

FIG. 1. (Color online) Polymers are free to diffuse within a tube formed by the surrounding network. Characteristic steps pointing in the directions {**u**} are randomly oriented under zero shear, though when the material is deformed (e.g., by a shear stress) the tubes are much more likely to have greater alignment with some preferred direction.

ditional precession $\omega(t)$ with respect to the Larmor frequency ω_0. In what follows we shall only consider this relative behavior of the spin precession.

By its equilibration motion, a polymer is free to take on any conformation within a tube which naturally lies between restrictions formed by contiguous tube steps characteristically traversing the distance a between entanglements, but which in thermal equilibrium are randomly oriented. Each step is also labelled with a normalized vector $\hat{\mathbf{u}}$ indicating its direction [see Fig. 1],

$$\hat{\mathbf{u}} = \begin{pmatrix} \sin\theta\cos\phi \\ \sin\theta\sin\phi \\ \cos\theta \end{pmatrix}, \tag{3}$$

where the spherical polar angles are measured with reference to the magnetic field frame as the z axis, and some arbitrary perpendicular direction as the x axis, a reference frame we shall later refer to as the $\{x,y,z\}$ or simply the laboratory frame. The laboratory frame defines the magnetic field direction and the magnetic field direction defines the secular part (projection) of the Hamiltonian which is expressed in Eq. (2). Ultimately it is against the laboratory frame $\{x,y,z\}$ that any such Hamiltonian projections will be made in our simulations and experiments.

Because the equilibration modes allow monomers to tumble at rates much faster than the dipole interaction strength the dipolar interaction is "preaveraged" within the local constraining tube step. It is these residual dipolar interactions that will allow investigation into slow polymer dynamics by NMR. Let the angles (θ,ϕ) denote the orientation of the tube step vector, **u**, with respect to the magnetic field and $(\Theta_{\mathbf{u}},\Phi_{\mathbf{u}})$ the orientation of the fluctuating internuclear vector with respect to **u**. Then, under motional averaging conditions, and by the spherical harmonic addition theorem, it may be shown

$$P_2[\cos\Theta(t)] = \langle P_2[\cos\Theta_{\mathbf{u}}(t)]\rangle P_2[\cos\theta(t)]. \tag{4}$$

Preaveraging results in $\langle P_2[\cos\Theta_{\mathbf{u}}(t)]\rangle$ being small but finite, leading to an effectively scaled dipolar interaction strength determined by the local value of $P_2[\cos\theta(t)]$, where we note that $\cos\theta(t)=\hat{u}_z(t)$. Allowing for this scaling effect we may write

$$\omega(t) = \omega_d\left[\hat{u}_z^2(t) - \tfrac{1}{3}\right]. \tag{5}$$

As the polymer reptates within the tube, the segments experience the stochastic fluctuations which arise from different projections, $\hat{u}_z(t)$ of the local tube directors. This leads us to describe $\omega(t)$ in terms of its two-point correlation function

$$C(t) = \langle\omega(t)\omega(0)\rangle \tag{6}$$

and its initial value ω_d^2.

Up to this point we have considered only a local spin pair experiencing dipolar interactions. Despite this, ω_d can encompass multiple dipolar interactions, whether intramolecular or intermolecular, so that ω_d represents the rms intensity of the combined set of dipolar interactions. It seems reasonable to assume that reptation will cause similar fluctuations in both intramolecular and intermolecular components. It is important to note that motional averaging, expressed through Eq. (4), causes the effective direction of the dipolar interaction to be successively projected. This means that for all fluctuations faster than the strength of the dipolar interaction (i.e., all internal segmental motion of the polymer) cause the effective internuclear axis to be tube step direction (see Fig. 1).

It is important to note that even allowing for multiple spin interactions, the scaled interaction strength ω_d will not be identical in each tube step because the distribution of lengths of subchains in each tube step will be Gaussian. It may be shown [15,16] that the dipolar interaction strength for a random coil subchain of K Kuhn segments of length b and end-to-end length r_K is given by $\omega_d=r_K^2(Kb^2)^{-1}\omega_{d0}$, where ω_{d0} is the root mean square $\overline{\omega_d^2}^{1/2}$ of the distribution of dipolar interaction strengths.

The probability distribution $P(r_K)\sim r_K^2\exp\left(-\frac{3r_K^2}{2Kb^2}\right)$ fully determines the probability distribution $P(\omega_d)$ of dipolar interaction strengths felt, whether arising from intramolecular or intermolecular interactions. This effect will need to be accounted for in our theory of dipolar interaction fluctuations.

2. The dipolar correlation and transverse relaxation in the Doi-Edwards De Gennes model

The NMR transverse relaxation experiment to be described here was carried out using a spin-echo sequence which has the effect of refocussing all unwanted magnetic field inhomogeneity whose Hamiltonian terms are all linear in the spin operators, while leaving unaffected the bilinear dipole-dipole interaction. What is measured therefore is

$$R(\tau) = \left\langle \exp\left\{ i \int_0^\tau dt' \, \omega(t') \right\} \right\rangle. \tag{7}$$

Following the work of Anderson and Weiss, in which it is assumed that the distribution of frequencies that have arisen due to dipolar fluctuations is Gaussian for certain classes of experiment the normalized transverse relaxation function for a single proton located in a tube segment which provides a certain remnant dipolar interaction strength may be written as [17]

$$R(\tau;\omega_d) = \exp\left(- \int_0^\tau dt' (\tau - t') C(t') \right). \tag{8}$$

Now the NMR signal enveloped by the total relaxation can be determined by summing the signals from all protons, which experience a range of dipolar interaction strengths

$$S(\tau) = \int_0^\infty d\omega_d R(\tau;\omega_d) P(\omega_d). \tag{9}$$

Clearly evaluation of $C(t')$ is the crucial step for any model of the dynamics. In the present case we may combine Eqs. (5) and (6) to write

$$C(t') = \omega_d^2 \left[\langle \hat{u}_z^2(t') \hat{u}_z^2(0) \rangle - \tfrac{2}{3} \langle \hat{u}_z^2(0) \rangle + \tfrac{1}{9} \right], \tag{10}$$

where we have assumed stationarity, $\langle \hat{u}_z^2(t') \rangle = \langle \hat{u}_z^2(0) \rangle$, and also that the local interaction strength ω_d is unchanged from time 0 to t. Strictly, ω_d will change over a Rouse time, as local polymer segments reptate. Our analysis suggests that allowing for this variation is of minor significance in comparison with allowance for the overall distribution in ω_d values.

Ball, Callaghan, and Samulski [13] adopted the Anderson-Weiss [18] approach to defining the relevant correlation function for the reptating polymer chains in terms of a return-to-origin probability. For the case where segments return to origin, $\langle \hat{u}_z^2(t') \hat{u}_z^2(0) \rangle = \langle \hat{u}_z^4(0) \rangle$ while otherwise $\langle \hat{u}_z^2(t') \hat{u}_z^2(0) \rangle = \langle \hat{u}_z^2(t') \rangle \langle \hat{u}_z^2(0) \rangle = \langle \hat{u}_z^2(0) \rangle^2$. The Doi-Edwards model gives us the means by which the RTO probability may be estimated for entangled high molecular mass polymers. We may estimate the chance that by curvilinear diffusion a certain monomer will return after a time delay t, to exactly the same tube step it originally occupied at time $t=0$, provided that tube step is not yet annihilated due to reptation. This probability, denoted $\Psi_{\mathrm{RTO}}(t)$, can be approximated by the values [13]

$$\Psi_{\mathrm{RTO}}(t) = \begin{cases} (t/\tau_e)^{-1/4}, & \tau_e < t < \tau_R, \\ (t/\tau_e)^{-1/4} (t/\tau_R)^{-1/4}, & \tau_R < t < \tau_d. \end{cases} \tag{11}$$

These $t^{-1/4}$ and $t^{-1/2}$ scaling regimes are related to well-known power-law signatures for reptation [20].

Clearly, any estimation of $C(t')$ concerns two probabilities, the RTO probability and the probability that a tube for a given polymer as seen from the reference state still exists. For a polymer segment to return to the initial tube step with the same director, the probability is $\psi_{\mathrm{tube}} \Psi_{\mathrm{RTO}}$ and $u_z^2(t) = u_z^2(0)$. Note the need for ψ_{tube} in the product, the requirement that the tube survives. Conversely the probability that the monomer ends up in a different environment step is $1 - \psi_{\mathrm{tube}} \Psi_{\mathrm{RTO}}$. This complementary probability allows for correlation loss due to either tube decay or to a failure for a monomer to return to origin, and should either of these two negative results occur, $\hat{u}_z^2(t)$ will be uncorrelated with $\hat{u}_z^2(0)$, causing $\langle \hat{u}_z^2(t) \rangle = \langle \hat{u}_z^2(0) \rangle$.

The correlation can hence be written as the weighted sum

$$C(t) = \omega_d^2 A \psi_{\mathrm{tube}}(t) \Psi_{\mathrm{RTO}}(t) + \omega_d^2 B [1 - \psi_{\mathrm{tube}}(t) \Psi_{\mathrm{RTO}}(t)] \tag{12}$$

$$= \omega_d^2 [(A - B) \psi_{\mathrm{tube}}(t) \Psi_{\mathrm{RTO}}(t) + B], \tag{13}$$

where following Eq. (10),

$$A = \langle \hat{u}_z^4(0) \rangle - \tfrac{2}{3} \langle \hat{u}_z^2(0) \rangle + \tfrac{1}{9}, \tag{14}$$

$$B = \langle \hat{u}_z^2(0) \rangle^2 - \tfrac{2}{3} \langle \hat{u}_z^2(0) \rangle + \tfrac{1}{9}. \tag{15}$$

In thermal equilibrium the distribution of $\mathbf{u}$ vectors is isotropic, $\langle \hat{u}_z^2(0) \rangle = \frac{1}{3}$ and $B=0$. Note the probability that the tube existing at time zero has survived until time t is denoted $\psi_{\mathrm{tube}}(t)$, a well-known, multiexponential function of time [7],

$$\psi_{\mathrm{tube}}(t) = \sum_{p \ \mathrm{odd}} \frac{8}{\pi^2 p^2} \exp\left(\frac{-p^2 t}{\tau_d} \right), \tag{16}$$

where τ_d is the tube disengagement time.

B. Dipolar relaxation function for reptating polymer segments in the presence of shear

1. Shear deformation tensor in the hydrodynamic frame

To handle the case where the polymer melt is continuously deformed, we make the assumption that the tube segments in the original melt hold a 1-1 correspondence with the tube segments in the resultant state. Typically the directions of the vectors along the tube segments are modified, though we still require that the new directors $\{\hat{\mathbf{u}}\}$ be normalized.

It is important to note that we assume that only the tube segments enveloping the actual polymer are deformed and biased in direction, and that no modification of local polymer dynamics occurs.

In a prototypical situation which can be related in the laboratory to a Couette shearing cell, for example, we can associate the X (or velocity) direction with the shear direction, where the Y and Z directions are the velocity gradient and vorticity directions, respectively. In this hydrodynamic frame $\{X, Y, Z\}$, arbitrary displacements and velocities are

transformed from their static counterparts through the application of the deformation tensor,

$$\underline{\underline{\mathbf{E}}}(\gamma) = \begin{pmatrix} 1 & \gamma & 0 \\ 0 & 1 & 0 \\ 0 & 0 & 1 \end{pmatrix}. \tag{17}$$

We shall be particularly interested in applying this tensor to the unit vectors representing tube segment directors. These directors $\mathbf{u}$ must be expressed in the $\{X,Y,Z\}$ frame, which for the three cases in which one of the three hydrodynamic axes are aligned with the z direction (the NMR B_0 field direction) can be obtained by a simple cyclical interchange of components,

$$\hat{u}_z'^2 = \hat{u}_{\{X,Y,Z\}}'^2 = \frac{(\underline{\underline{\mathbf{E}}} \cdot \hat{\mathbf{u}})^2_{\{X,Y,Z\}}}{\|\underline{\underline{\mathbf{E}}} \cdot \hat{\mathbf{u}}\|^2} \equiv h_{\{X,Y,Z\}}(\gamma,\theta,\phi). \tag{18}$$

Following Doi and Edwards [7] we assign the effective strain γ to the Weissenberg number $\dot{\gamma}\tau_d$, where $\dot{\gamma}$ is the steady shear rate.

2. The correlation function under shear

Should a shear field (or other deformational flow) be imposed upon the polymer the transformed and renormalized directors are substituted with no further modification to this expression, due to the 1-1 correspondence between tube steps in the thermal equilibrium and flow deformed distributions. We may now use this expression for h in the equations for A and B,

$$A(\gamma) = \langle h^2(\gamma,\theta,\phi)\rangle - \tfrac{2}{3}\langle h(\gamma,\theta,\phi)\rangle + \tfrac{1}{9}, \tag{19}$$

$$B(\gamma) = \langle h(\gamma,\theta,\phi)\rangle^2 - \tfrac{2}{3}\langle h(\gamma,\theta,\phi)\rangle + \tfrac{1}{9}. \tag{20}$$

Unlike the zero shear case $B \neq 0$. From Eq. (12),

$$R(\tau;\omega_d) = \exp\left\{-\omega_d^2 \int_0^\tau dt(\tau - t)[(A-B)\psi_{\text{tube}}(t)\Psi_{\text{RTO}}(t) + B]\right\}. \tag{21}$$

This is an expression involving an integral which we expect to be simple to evaluate numerically—given that we have calculated A and B for an experiment conducted at a given shear rate previously. The $\dot{\gamma}\tau_d$-dependence inherited from A and B is implicit in the calculation.

C. Predictions for magnetic field along vorticity, gradient, and velocity directions

In the NMR experiment the z axis is defined by the magnetic field direction. In Doi-Edwards theory the $\{X,Y,Z\}$ axes refer to the hydrodynamic frame. In practice we may select different axes in this frame via the magnetic field, by simply choosing our sample geometry appropriately. For example, we may choose $z \equiv Z$ by using a Couette cell geometry which is aligned with the NMR B_0 field (the vertical Couette). In this case the relevant projection of h is h_Z. Through the use of a "slice-selection" technique in which a signal may be acquired from a predetermined segment of the sample, a horizontal Couette can be used as shown in Fig. 2 so that the NMR B_0 field is projected along X or Y for the chosen segment. We now undertake to find expressions for h_X and h_Y.

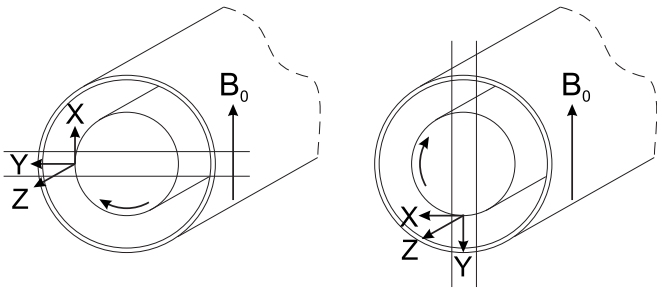

FIG. 2. Simulating the NMR signal where the velocity direction X is aligned with the magnetic field is experimentally equivalent to restricting the active volume of a horizontal Couette cell to lie in the horizontal plane (left of figure), and (right of figure) vertical slice selection on a Couette cell is matched theoretically by the simulation $z \equiv Y$.

1. Velocity direction=B_0 direction

Focussing now on the case where the shear direction is coincident with the B_0 field direction, we should note that we will still use the same deformation tensor (i.e., the one that produces the transformation $X \to X + \gamma Y$ in the hydrodynamic frame), but the components of $\hat{\mathbf{u}}$ will be cyclicly interchanged in correspondence with the axes. In this geometry ($X \equiv z$, $Y \equiv x$, $Z \equiv y$), then, $u_z \to u_z + \gamma u_x$, and the deformation tensor equation reads

$$\underline{\underline{\mathbf{E}}} \cdot \hat{\mathbf{u}} = \begin{pmatrix} 1 & \gamma & 0 \\ 0 & 1 & 0 \\ 0 & 0 & 1 \end{pmatrix} \begin{pmatrix} \cos\theta \\ \sin\theta\cos\phi \\ \sin\theta\sin\phi \end{pmatrix},$$

$$(\underline{\underline{\mathbf{E}}} \cdot \hat{\mathbf{u}})_z^2 = (\underline{\underline{\mathbf{E}}} \cdot \hat{\mathbf{u}})_X^2 = (\cos\theta + \gamma\sin\theta\cos\phi)^2,$$

$$\|\underline{\underline{\mathbf{E}}} \cdot \hat{\mathbf{u}}\|^2 = 1 + \gamma\cos\phi\sin 2\theta + \gamma^2\sin^2\theta\cos^2\phi, \tag{22}$$

and hence from Eq. (18)

$$h_X(\gamma,\theta,\phi) = \frac{(\cos\theta + \gamma\sin\theta\cos\phi)^2}{1 + \gamma\cos\phi\sin 2\theta + \gamma^2\sin^2\theta\cos^2\phi}. \tag{23}$$

2. Velocity gradient direction=B_0 direction

We turn now to the final case which is orthogonal to the NMR frame, that in which the velocity gradient direction is coincident with the B_0 field. Again we use the same deformation tensor ($X \to X + \gamma Y$ in the hydrodynamic frame), and the components of $\hat{\mathbf{u}}$ will be cyclicly interchanged once more, such that $u_y \to u_y + \gamma u_z$, and the deformation tensor equation now reads

$$\underline{\underline{\mathbf{E}}} \cdot \hat{\mathbf{u}} = \begin{pmatrix} 1 & \gamma & 0 \\ 0 & 1 & 0 \\ 0 & 0 & 1 \end{pmatrix} \begin{pmatrix} \sin\theta\sin\phi \\ \cos\theta \\ \sin\theta\cos\phi \end{pmatrix} \tag{24}$$

and similarly

$$(\underline{\underline{\mathbf{E}}} \cdot \hat{\mathbf{u}})_z^2 = (\underline{\underline{\mathbf{E}}} \cdot \hat{\mathbf{u}})_Y^2 = \cos^2\theta,$$

$$\|\underline{\underline{\mathbf{E}}} \cdot \hat{\mathbf{u}}\|^2 = 1 + \gamma \sin\phi \sin 2\theta + \gamma^2 \cos^2\theta$$

and hence from Eq. (18),

$$h_Y(\gamma, \theta, \phi) = \frac{\cos^2\theta}{1 + \gamma \sin\phi \sin 2\theta + \gamma^2 \cos^2\theta}. \tag{25}$$

III. EXPERIMENT

A. Horizontal Couette measurement of T_2 in polymer melts

As explained in the introduction, the purpose of the present work is to use proton NMR transverse relaxation to measure segmental alignment under shear, thus circumventing the need for a deuterated probe molecule and the consequently lower signal-to-noise ratio. The through-space dipolar interactions between protons are analogous to the deuteron's electric quadrupolar interaction with the molecular bond electron cloud, so that the physics expressed by Eq. (2) apply in each case. The distribution of dipolar interaction strengths leads to a loss of phase coherence of the spin system and a damping of the signal, the so-called T_2 relaxation. To remove unwanted damping effects due to local field inhomogeneity, we utilize a spin-echo to measure T_2. Under the spin-echo, magnetic terms in the spin Hamiltonian are refocussed, while dipolar terms remain.

NMR spectra and the extracted values for the characteristic transverse relaxation time T_2 were all obtained through the use of a horizontal Couette cell located within the bore of a Bruker AMX 300 MHz wide bore magnet. The sample used was a high molecular weight (M_p=494 kDa) poly(dimethylsiloxane) (or PDMS) (see Fig. 3) with a polydispersity index M_w/M_n=1.84, obtained from American Polymer Standards Corporation. PDMS has a glass transition temperature of approximately −150 °C [19], well below room temperature, and its structure (see Fig. 3) is such that both intramolecular and intermolecular proton dipolar interactions play a role in the melt. The molecular weight located between entanglements M_e in such a PDMS melt is ~10 kDa [19] and hence the number of entanglements Z along the length of the polymer is simply $M/M_e \sim 49$. The flow curve of this polymer is shown in Fig. 4 with both shear stress and normal stresses indicated.

The poly(dimethylsiloxane) is enclosed in a 0.5 mm gap between concentric MACOR machinable glass tubes (Corning, NY). By using slice-selective gradients, only specific volumes within the sample that highlight the regions of interest (e.g., velocity direction aligned with NMR B_0 field) are active in the experiment. This was achieved through the use of a sequence (90°_x-τ-180°_y-τ-acquire), shown schematically in Fig. 5. The selective excitation pulse sequence used has been specially devised to minimize exposure of selected nuclear spins to any relaxation, so that high quality NMR spectroscopy can be performed in the desired region. We describe this method in another paper [9], however the essential details of the pulse and the Couette are shown in Figs. 5 and 6. The technique employs a selective precursor pulse sandwich which destroys magnetization outside the desired region but which stores along the z axis for later recall, the magnetization from the region of interest. Using a variant of the pulse sequence of Fig. 5 this magnetization can be used to obtain a confirmatory image (see Fig. 7). Experiments were carried out with an acquisition bandwidth of 50 kHz and 102 different delay times τ were used between 0.1 ms and 300 ms. The duration of the slice selective pulse is of the order of 1 ms so that insignificant slice distortion occurs due to shear. Furthermore, motion during the spin-echo does not significantly perturb the shear-dependent dipolar interactions due to the small proportion of fluid experiencing high velocity near the inner wall [4].

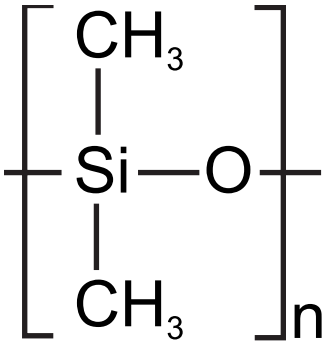

FIG. 3. The chemical structure of poly(dimethylsiloxane).

B. Numerical computation of T_2 in polymer melts

Our numerical calculations based on the theory described previously were all performed by software hand-coded in C++. The software allows the choice of orientation of the

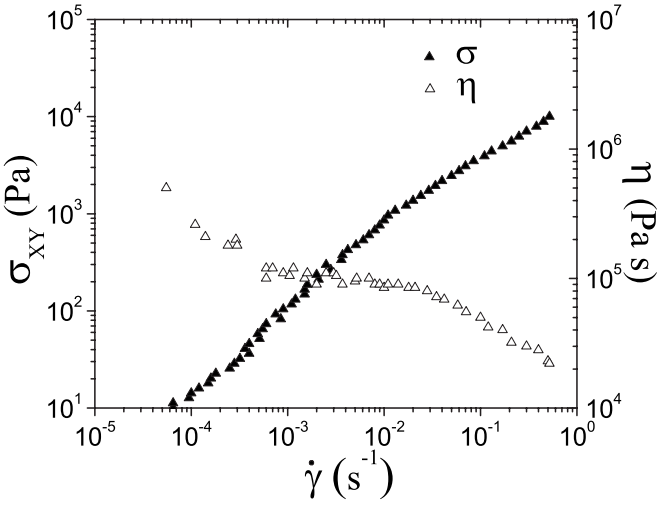

FIG. 4. Flow curve for the PDMS sample used in all experiments.

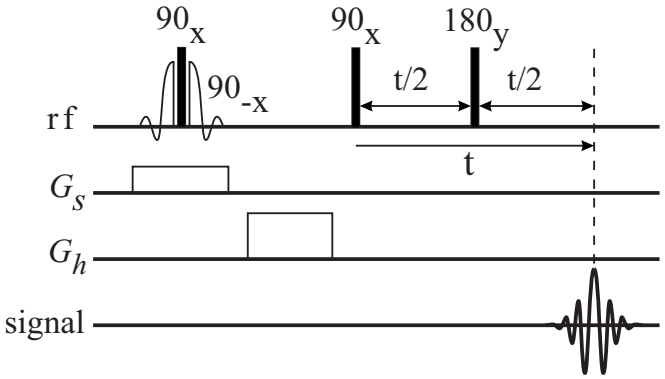

FIG. 5. The Hahn echo pulse program, which consists of a preliminary pulse sandwich which leaves only longitudinal signal from a desired slice (achieved by applying a slice gradient G_s, followed by a transverse magnetization-destroying homospoil gradient G_h), followed by a standard echo sequence of varying echo time. The signal strength as a function of echo time yields T_2.

Couette cell, as well as shear rate, the two free parameters for the laboratory experimenter to change, in addition to tunable parameters particularly relevant to the sample being investigated, namely the tube disengagement time τ_d, the average dipole interaction strength ω_{d0}, and Z, the number of tube segments the polymer is divided into by entanglements.

Given the orientation and shear rate, it is a simple matter to evaluate the relevant $h_{\{X,Y,Z\}}$ function, and hence find A and B. The modification of Eq. (8) is appropriate at this stage so as to accommodate our expectation that the distribution of dipolar interaction strengths is not unimodal, but is spread broadly due to the end-to-end vector of local subchains in each tube being Gaussian. The double integral over ω_d and t can now be evaluated to determine the normalized transverse relaxation function desired.

IV. RESULTS AND DISCUSSION

Experimental measurement of T_2 in polymer melts, and fitting model parameters

Using the Hahn echo pulse sequence previously described, the echo signal acquired is modulated by the transverse relaxation envelope. Plotted on a logarithmic scale, all echo signal intensities acquired at shear rates ranging from 0 to 100 s^{-1} are closer to Lorentzian $[S(t) \sim \exp(-kt)]$ than Gaussian $[S(t) \sim \exp(-kt^2)]$, as seen in Fig. 8. By making a Taylor expansion of the return-to-origin probabilities in Eq. (8), it can be seen that if the problem were treated with a unique value of the preaveraged dipolar interaction strength, a Gaussian line shape might be expected. However, by performing the integral over the correct weighting of ω_d values a line shape closer to Lorentzian results. Note however that for very short times, the theory (see Fig. 9) does predict an opposite curvature to that seen in the measurements. One possible explanation for the initial rapid decay of the measured signal is the settling of the spin-echo to steady state under the action of a less than perfect 180° refocussing radio-frequency pulse.

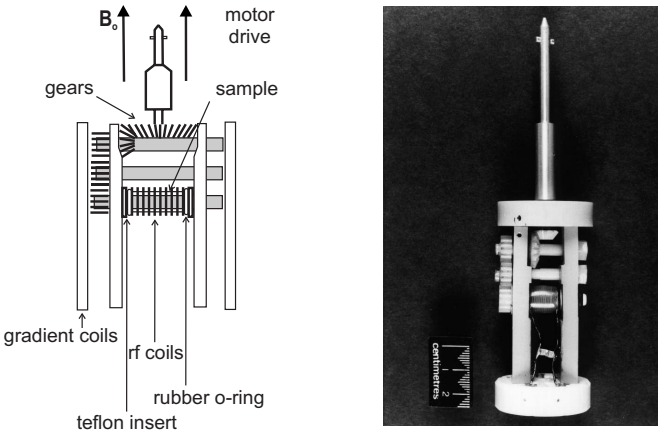

FIG. 6. The horizontal Couette cell.

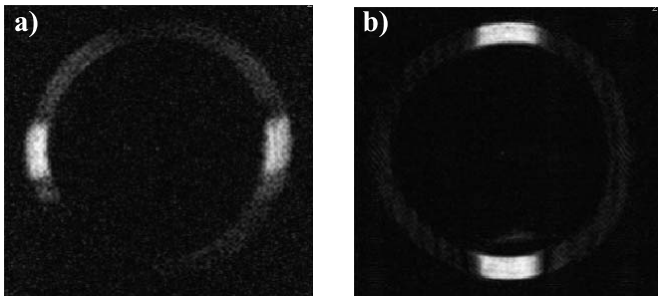

FIG. 7. (a) Slice of active volume produced in a horizontal Couette cell (viewed along the cell vorticity axis) by applying a z gradient in the pulse program, and (b) an alternate active volume produced by applying a gradient perpendicular to the z direction and the vorticity axis of the cell.

Figure 10 shows the extraction of $1/e$ points from these acquired curves as a function of shear rate. From this data, T_2 appears to be heavily shear-rate-dependent at low $(\dot{\gamma} < 20)$ shear rates before finding an ultimate T_2 at higher shear rates, where little or no further decrease is seen.

In fitting the three tunable parameters Z, ω_{d0}, and τ_d, three characteristic reference conditions were used, namely the transverse relaxation times at $\dot{\gamma}=0$ s^{-1}, $\dot{\gamma}=10$ s^{-1}, and $\dot{\gamma}=100$ s^{-1}. With the preliminary values of $Z=50$, $\tau_d=210$ ms, chosen from earlier work [11], the ratio of the transverse relaxation time at low and high shear rates was found to be disproportionately large and hence these values were adjusted to give a best fit between experimental values of T_2 and numerical simulation. We obtain

$$Z = 35 \pm 10,$$

$$\omega_{d0} = (3900 \pm 200)\ \text{Hz},$$

$$\tau_d = (600 \pm 300)\ \text{ms}.$$

We note immediately that the value of ω_{d0} obtained here is consistent with that found in earlier equilibrium studies [3], noting that in that reference, $M_2 = A\omega_{d0}^2$, where in equilibrium, $A = 4/45$. By contrast the values of Z and τ_d differ

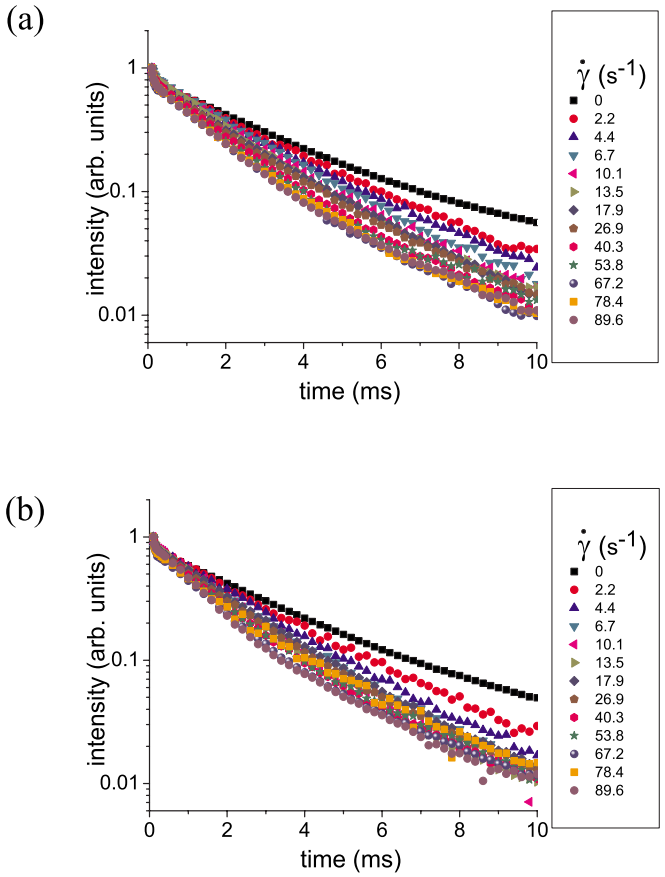

FIG. 8. (Color online) (a) Experimentally measured echo signals, having obtained a horizontal slice within the horizontal Couette geometry ($z \equiv X$) for different shear values, and (b) those signals obtained through the use of a vertical slice.

somewhat from values obtained using deuterium NMR ($Z \sim 49$, $\tau_d = 210$ ms) [11]. This is perhaps not surprising given the very different nature of the averaging processes relevant to deuterium NMR (where the probe molecule motionally averages the segment ensemble) and proton NMR (in which a sum of signals arising from different segments is averaged). We note that the sample has finite polydispersity $\left(\frac{M_w}{M_n} = 1.84\right)$ and no distribution of molecular weights has been allowed for in our simulation, nor was it considered in the earlier deuterium NMR work.

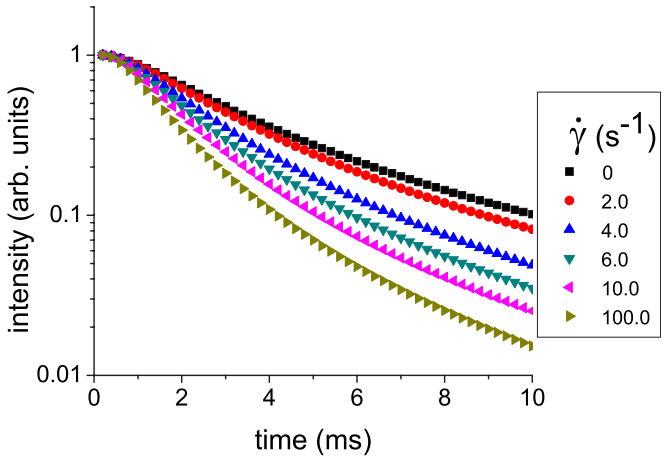

FIG. 9. (Color online) Simulated echo signals for the horizontal Couette geometry ($z \equiv X$) for different shear values.

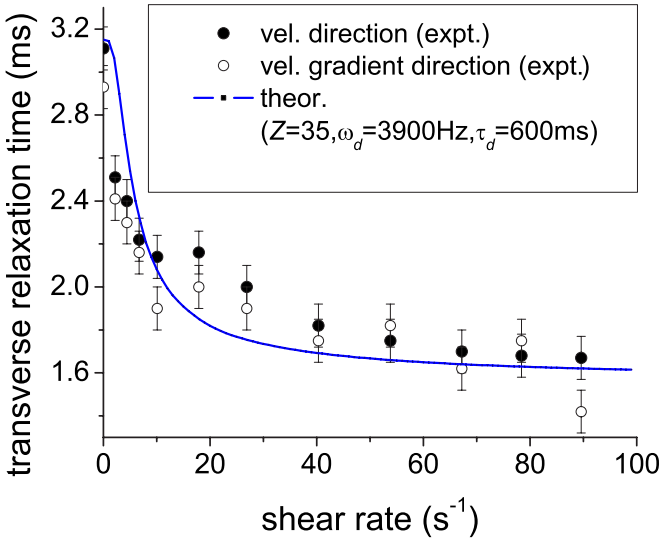

FIG. 10. (Color online) Simulated transverse relaxation time as a function of shear rate, in the cases where the hydrodynamic X axis and the hydrodynamic Y axis are aligned with the magnetic field B_0. The data points correspond to $1/e$ times obtained for the echo attenuation at different shear rates.

With our best-fit values, the signals generated for the horizontal Couette cell experiment [i.e., using the h_X expression in the $AB(\gamma)$ function] are shown in Fig. 9 for shear rates varying between 0 and 100 s^{-1}. The curve corresponding to a shear rate of 100 s^{-1} is essentially the infinite shear case: increasing shear does not modify the curve further. It is also interesting to note that at all shear rates the difference in transverse relaxation time between the h_X and h_Y cases is at most 0.1%.

V. CONCLUSIONS

Using the observation of proton NMR transverse relaxation, we have seen the effects of shear induced alignment in polymer melts. In order to understand these effects we have developed further a theory of proton relaxation based on the Doi-Edwards framework, in particular focussing on the time-correlated probability that a proton attached to a polymer chain returns to the same tube segment through reptation. The effect of shear is to perturb the orientational distribution of tube steps, and so to influence the dipolar correlation function. A key aspect is the inclusion of a distribution of dipolar interaction strengths ω_d, thus explaining near Lorentzian signal decay. We are thus able to measure T_2 values for a 494 kDa melt of poly(dimethylsiloxane).

The theory broadly matches the time dependence of the echo decays, and the dependence of T_2 values on shear rate.

A fit to the shear dependent T_2 data yields the values $\tau_d = 600$ ms, $Z = 35$ and $\omega_{d0} = 3900$ Hz. The Z and τ_d values are consistent with earlier measurements made using deuterium NMR under shear, while the fitted value for ω_{d0} is consistent with proton dipolar relaxation measurements under zero shear.

ACKNOWLEDGMENTS

The authors acknowledge financial support from the Royal Society of New Zealand Marsden Fund and Centres of Research Excellence Fund. The authors are grateful to Dr. Siegfried Stapf for useful discussions, and to Professor Ed Samulski for many illuminating insights.

[1] A. I. Nakatani, M. D. Poliks, and E. T. Samulski, Macromolecules **23**, 2686 (1990).
[2] A. Gottwald and U. Scheler, Polym. Prepr. (Am. Chem. Soc. Div. Polym. Chem.) **44**, 273 (2003).
[3] P. T. Callaghan and E. T. Samulski, Macromolecules **31**, 3693 (1998).
[4] J. M. Atkin, R. J. Cormier, and P. T. Callaghan, J. Magn. Reson. **172**, 91 (2005).
[5] S. Hofl, F. Kremer, H. W. Spiess, M. Wilhelm, and S. Kahle, Polymer **47**, 7282 (2006).
[6] D. A. Grabowski and C. Schmidt, Macromolecules **27**, 2632 (1994).
[7] M. Doi and S. F. Edwards, *The Theory of Polymer Dynamics* (Clarendon, Oxford, 1986).
[8] G. Marrucci and G. Ianniruberto, J. Non-Newtonian Fluid Mech. **82**, 275 (1999).
[9] M. L. Kilfoil and P. T. Callaghan, Macromolecules **33**, 6824 (2000).
[10] R. J. Cormier, M. L. Kilfoil, and P. T. Callaghan, Phys. Rev. E **64**, 051809 (2001).
[11] R. J. Cormier and P. T. Callaghan, J. Chem. Phys. **116**, 10020 (2002).
[12] C. P. Slichter, *Principles of Magnetic Resonance* (Springer-Verlag, New York, 1990).
[13] R. C. Ball, P. T. Callaghan, and E. T. Samulski, J. Chem. Phys. **106**, 7352 (1997).
[14] M. Doi and S. F. Edwards, J. Chem. Soc., Faraday Trans. 1 **74**, 1802 (1978).
[15] B. Deloche and E. T. Samulski, Macromolecules **23**, 1999 (1990).
[16] P. Sotta and B. Deloche, Macromolecules **14**, 575 (1981).
[17] A. Abragam, *Principles of Nuclear Magnetism* (Clarendon, Oxford, 1961).
[18] P. W. Anderson and P. R. Weiss, Rev. Mod. Phys. **25**, 269 (1953).
[19] J. D. Ferry, *Viscoelastic Properties of Polymers* (Clarendon, Oxford, 1961).
[20] P.-G. De Gennes, J. Chem. Phys. **55**, 572 (1971).